Modified Bowtie Antenna for Zeroth Order Resonance

Thazhe K. Roshna, Unnimadhavan Deepak, Vallathadam R. Sajitha, Kesavath Vasudevan, and Pezholil Mohanan*

Abstract—A novel extremely compact Zeroth Order Resonator (ZOR) antenna with a chip inductor, for Digital Video Broadcasting-Handheld (DVB-H) application, is presented. The proposed antenna has a bowtie structure with an overall dimension of $0.0186\lambda_0 \times 0.020\lambda_0 \times 0.003\lambda_0\,\text{mm}^3$ at 503 MHz. The zeroth resonance property makes the resonant frequency to be independent of the antenna dimension. The 3 : 1 VSWR bandwidth of the antenna is 39 MHz and offers an omnidirectional radiation pattern. A 99.1% reduction in the overall area of the structure is achieved compared to a conventional circular patch antenna operating at the same frequency.

1. INTRODUCTION

The rapid development of various wireless protocols increases the needs for antennas having low profile, compact size and light weight with ease of fabrication. Many techniques have been developed to achieve compactness in the antenna design such as integrating shorting walls on the radiating element, using stacked structures and fractal geometries [1–4]. Recently, Composite Right/Left Handed (CRLH) Transmission Lines (TLs), composed of shunt inductors and series capacitors periodically loaded along the host TLs, have drawn increasing attention because of its many unusual properties [5–7]. One of the unusual properties is the zeroth-order resonance at which the phase constant, β is zero for a non-zero frequency. This enables the resonant frequency to be independent of the antenna dimension [8–10]. A 75% reduction in the footprint area of the structure can be achieved compared to a conventional patch antenna by using meander-line inductor [11]. In CRLH TLs, the quasi lumped-element implementation of shunt inductance and series capacitance are obtained by vias to ground plane and inter-digital capacitors respectively [12]. This makes the fabrication difficult and tedious. In [13, 14], a chip inductor was embedded in the printed monopole antennas, which results in a decrease in the resonant length of the fundamental mode.

In this paper a novel Zeroth Order Resonant Antenna (ZORA) using a chip inductor is proposed. The chip inductor reduces the overall antenna size. Here the unique property of the CRLH TLs, i.e., zeroth order resonance, is accomplished on a bowtie structure, since it is simple to fabricate. The features of the bowtie include wider bandwidth, higher gain, lower front-to-back ratio, lower cross-polarization level and smaller size [15]. A conventional CRLH TL is composed of a series inductance and capacitance as well as shunt inductance and capacitance. The zeroth-order mode is determined by the shunt components in the case of an open ended transmission line and by series components in short ended transmission line. By increasing the shunt inductance, the zeroth-order resonant frequency can be decreased, so that the antenna size can be made much smaller. In this proposed structure, the shunt inductance is accomplished by embedding a chip inductor on one of the strip of the bowtie antenna. Thus it omits the need for vias to the ground. The series capacitor of a traditional CRLH TL is taken away in order to reduce both size and structural complexity, which makes the system devoid of left-handed (LH) transmission but retaining the zeroth-order resonance and right-handed transmission [16].

Received 15 January 2014, Accepted 26 February 2014, Scheduled 5 March 2014
* Corresponding author: Pezholil Mohanan (drmohan@gmail.com).
The authors are with the Centre for Research in ElectroMagnetics and Antennas (CREMA), Department of Electronics, Cochin University of Science and Technology, Cochin 22, Kerala, India.

The proposed antenna with dimension $0.0186\lambda_0 \times 0.020\lambda_0 \times 0.003\lambda_0\,\text{mm}^3$ has a zeroth order resonance at 503 MHz, which makes it electrically very small [18], where λ_0 is the free space wavelength corresponding to the resonant frequency. In addition the high gain wide band of the original bowtie antenna at higher frequencies [15] is retained. The optimization of the antenna dimensions is carried out using Ansoft HFSS.

2. ANTENNA GEOMETRY AND DESIGN

Figure 1 shows the proposed bowtie antenna with an inductor. The prototype is fabricated on a substrate of relative permittivity (ϵ_r) 4.4 and thickness (h) 1.6 mm. The antenna requires a small footprint of $0.0186\lambda_0 \times 0.020\lambda_0 \times 0.003\lambda_0\,\text{mm}^3$ only.

A 0603CS 120 nH Coilcraft surface mount inductor is mounted on one of the arms of the bowtie antenna as shown in Figure 1. The effect of the loaded chip inductor is an increase in the electrical length of the bowtie antenna, and thus lowering the resonant frequency.

The circuit model of the proposed antenna is shown in Figure 2(a). The parasitic components can be modeled using series inductance (L_R) and shunt capacitance (C_R). The bow (flaring) corresponding to the inductor loaded strip, acts as a metal patch and provides a capacitance C_g to the ground. When C_g is large, it provides a virtual ground voltage [19, 20] and thus realizes the shunt inductance (L_L). This condition triggers the zeroth order mode of the structure at lower frequencies. At higher frequencies the virtual ground effect fails as the inductor impedance increases and results in the right-handed transmission. Figure 2(b) shows a schematic representation of the proposed dispersion diagram corresponding to the circuit model.

3. THEORY

The proposed antenna suppresses the left-handed transmission (phase advance) but possesses zero phase constant and right-handed transmission (phase delay) [6]. The suppression of LH transmission took place since there is no series capacitance (C_L) [16] as in Figure 2(a).

By applying boundary condition related to Bloch-floquet theorem [12] to the structure, the dispersion relation, $\beta(\omega)$, of the simplified TL in Figure 2(a) is obtained as

$$\beta(\omega) = \cos^{-1}\left(1 + \frac{ZY}{2}\right) \tag{1}$$

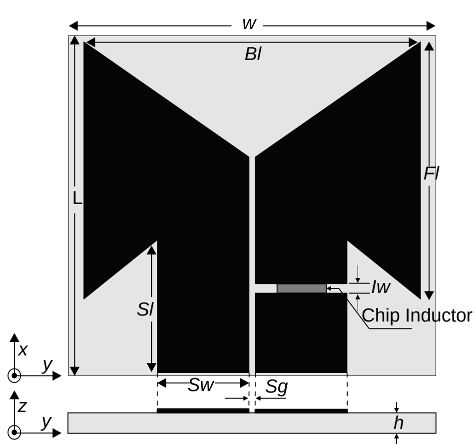

Figure 1. Geometry of proposed antenna, $Bl = 11\,\text{mm}$, $Fl = 8.4\,\text{mm}$, $Sl = 4\,\text{mm}$, $Sw = 3\,\text{mm}$, $Sg = 0.2\,\text{mm}$, $Iw = 0.3\,\text{mm}$, $h = 1.6\,\text{mm}$, $L = 11.1\,\text{mm}$, $W = 12\,\text{mm}$.

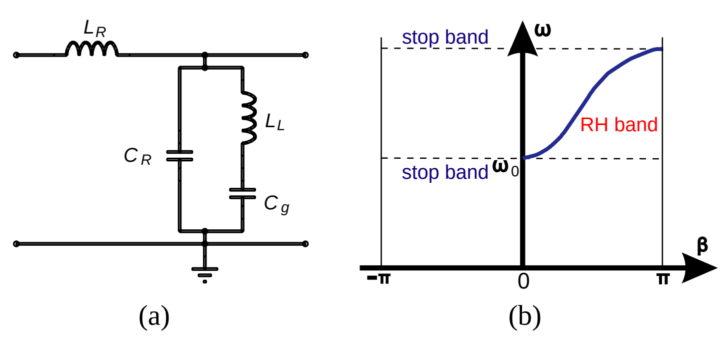

Figure 2. (a) Circuit model of bowtie ZORA. (b) Dispersion diagram.

where the series impedance (Z) and shunt admittance (Y) are given by

$$Z(\omega) = j(\omega L_R) \tag{2}$$

$$Y(\omega) = j\left(\omega C_R - \cfrac{1}{\omega L_L - \cfrac{1}{\omega C_g}}\right) \tag{3}$$

when $\omega L_L \gg \frac{1}{\omega C_g}$ then $Y(\omega)$ approaches the admittance of $L_L C_R$ tank resonator and therefore C_g has less influence on the propagation characteristics [18]. By applying Taylor series approximation, (1) becomes

$$\beta(\omega) = \sqrt{\omega^2 L_R C_R - \cfrac{L_R}{L_L - \cfrac{1}{\omega^2 C_g}}} \tag{4}$$

The propagation constant approaching zero results in the zeroth order resonance (or infinite wavelength resonance). Here the structure acts as an open ended transmission line, so the zeroth mode frequency is determined by shunt circuit [18].

$$\omega = \omega_0 = \sqrt{\omega_{sh}^2 + \omega_g^2} \tag{5}$$

where $\omega_{sh} = \frac{1}{\sqrt{L_R C_R}}$ and $\omega_g = \frac{1}{\sqrt{L_L C_g}}$.

As L_L, C_R and C_g are increased, the resonant frequency decreases. It is more effective to increase L_L rather than C_R and C_g, by simply increasing the value of the chip inductor. When L_L becomes larger, the zeroth-mode resonance shifts to lower frequency region, making the antenna more compact in size.

4. SIMULATION AND EXPERIMENTAL RESULTS

Agilent PNA E8362B network analyzer is used for experimental analysis. The proposed ZOR antenna with a 120 nH chip inductor was fabricated and measured. A photograph of the antenna is shown in Figure 3. Figure 4(a) shows the simulated and measured reflection coefficient as well as the transmission coefficient of the antenna. The slight discrepancy in the S_{11} curve is due to the coupling of the SMA connector, which is not considered in the simulation. Figure 4(b) depicts the comparison of reflection characteristics at higher frequency region, between the bowtie antennas with and without inductor. A bowtie antenna without embedding any chip inductor has only $n = +1$ mode. From Figures 4(a) & 4(b) it is clear that for the proposed antenna the higher resonance is still determined by the bowtie structure while the lower resonance is due to the presence of a 120 nH inductor. For this inductor-loaded antenna, $n = 0$ mode is the lowest mode, because it does not support backward wave like the CRLH TL. The $n = 0$ mode resonates at 503 MHz with a reflection coefficient of -35 dB and a 3 : 1 VSWR bandwidth of 39 MHz and for $n = +1$ mode the resonance is at 9.15 GHz with a reflection coefficient of -17 dB as shown in Figures 4(a) & 4(b).

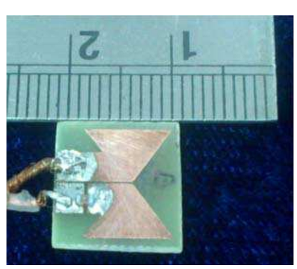

Figure 3. Photograph of the fabricated prototype, $Bl = 11$ mm, $Fl = 8.4$ mm, $Sl = 4$ mm, $Sw = 3$ mm, $Sg = 0.2$ mm, $Iw = 0.3$ mm, $h = 1.6$ mm, $L = 11.1$ mm, $W = 12$ mm.

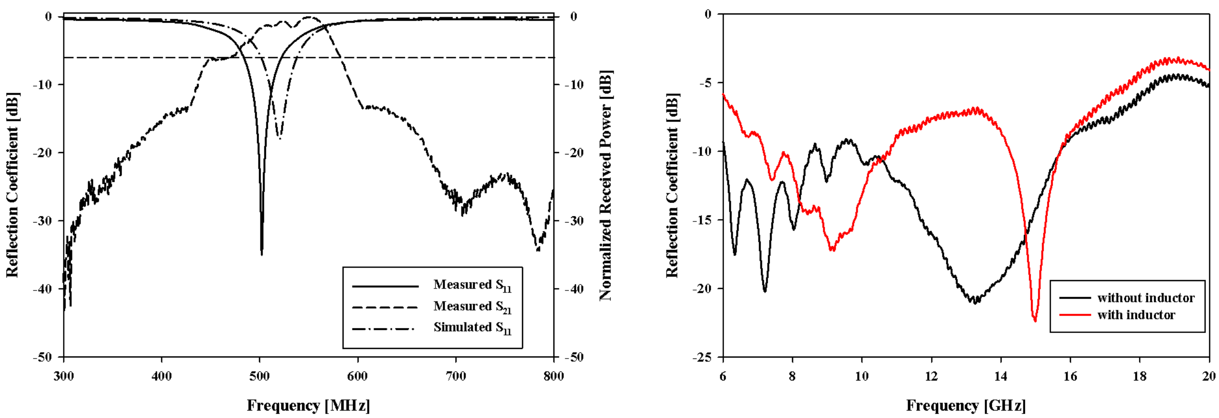

Figure 4. (a) Transmission and reflection characteristics of antenna. (b) Reflection coefficient of bowtie antenna with and without inductor, $Bl = 11$ mm, $Fl = 8.4$ mm, $Sl = 4$ mm, $Sw = 3$ mm, $Sg = 0.2$ mm, $Iw = 0.3$ mm, $h = 1.6$ mm, $L = 11.1$ mm, $W = 12$ mm.

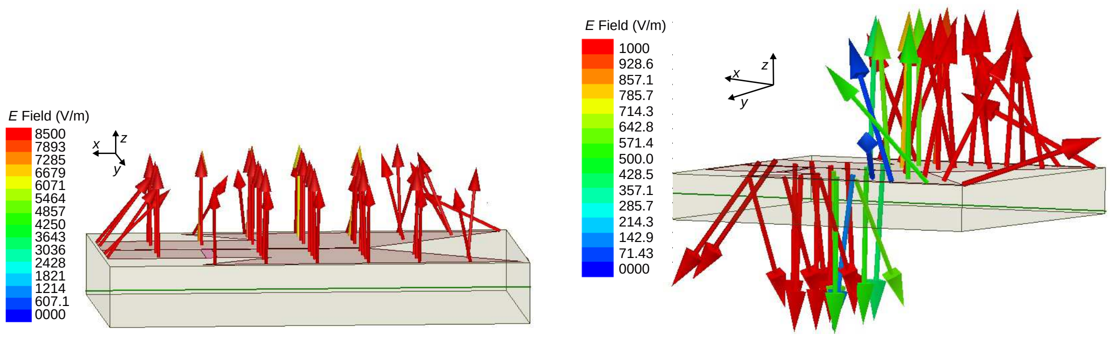

Figure 5. Electric field distribution, (a) at $n = 0$ mode, (b) at $n = +1$ mode, $Bl = 11$ mm, $Fl = 8.4$ mm, $Sl = 4$ mm, $Sw = 3$ mm, $Sg = 0.2$ mm, $Iw = 0.3$ mm, $h = 1.6$ mm, $L = 11.1$ mm, $W = 12$ mm.

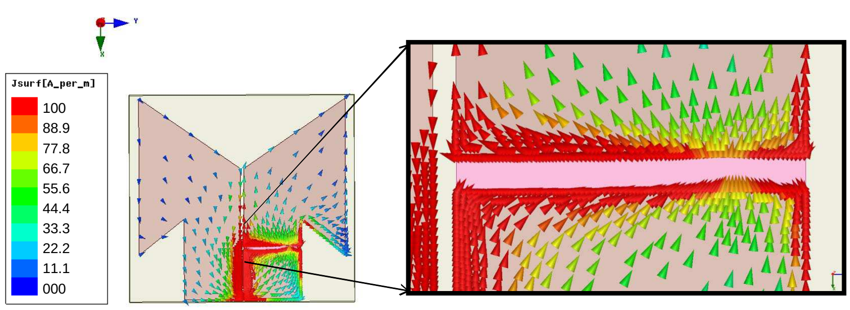

Figure 6. Surface current distribution at 503 MHz, $Bl = 11$ mm, $Fl = 8.4$ mm, $Sl = 4$ mm, $Sw = 3$ mm, $Sg = 0.2$ mm, $Iw = 0.3$ mm, $h = 1.6$ mm, $L = 11.1$ mm, $W = 12$ mm.

The electric field distribution for $n = 0$ ($\beta = 0$) and $n = +1$ ($\beta > 0$) are analyzed. At 503 MHz ($n = 0$) the electric fields are uniformly distributed and are in-phase as in Figure 5(a). This verifies the infinite wavelength resonance condition [16, 17]. While at 9.15 GHz ($n = +1$) the electric field is sinusoidally distributed and are out of phase corresponding to a half-wavelength, as in Figure 5(b). This shows the right-handed wave propagation through the structure. The surface current distribution on the antenna at 503 MHz is depicted in Figure 6. It is found that the surface current at the slot edges

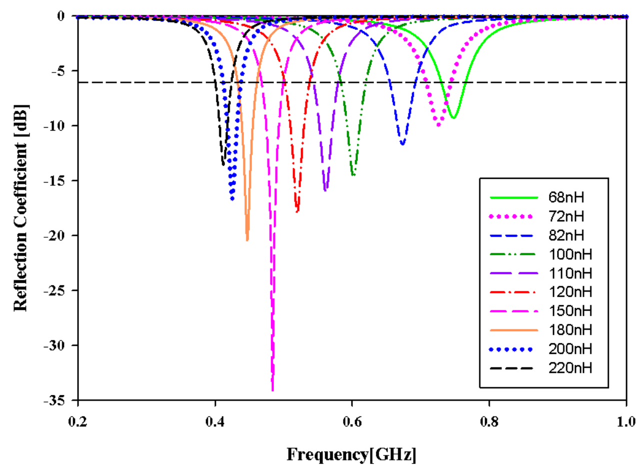

Figure 7. Resonant frequency variation with chip inductor value, $Bl = 11\,\text{mm}$, $Fl = 8.4\,\text{mm}$, $Sl = 4\,\text{mm}$, $Sw = 3\,\text{mm}$, $Sg = 0.2\,\text{mm}$, $Iw = 0.3\,\text{mm}$, $h = 1.6\,\text{mm}$, $L = 11.1\,\text{mm}$, $W = 12\,\text{mm}$.

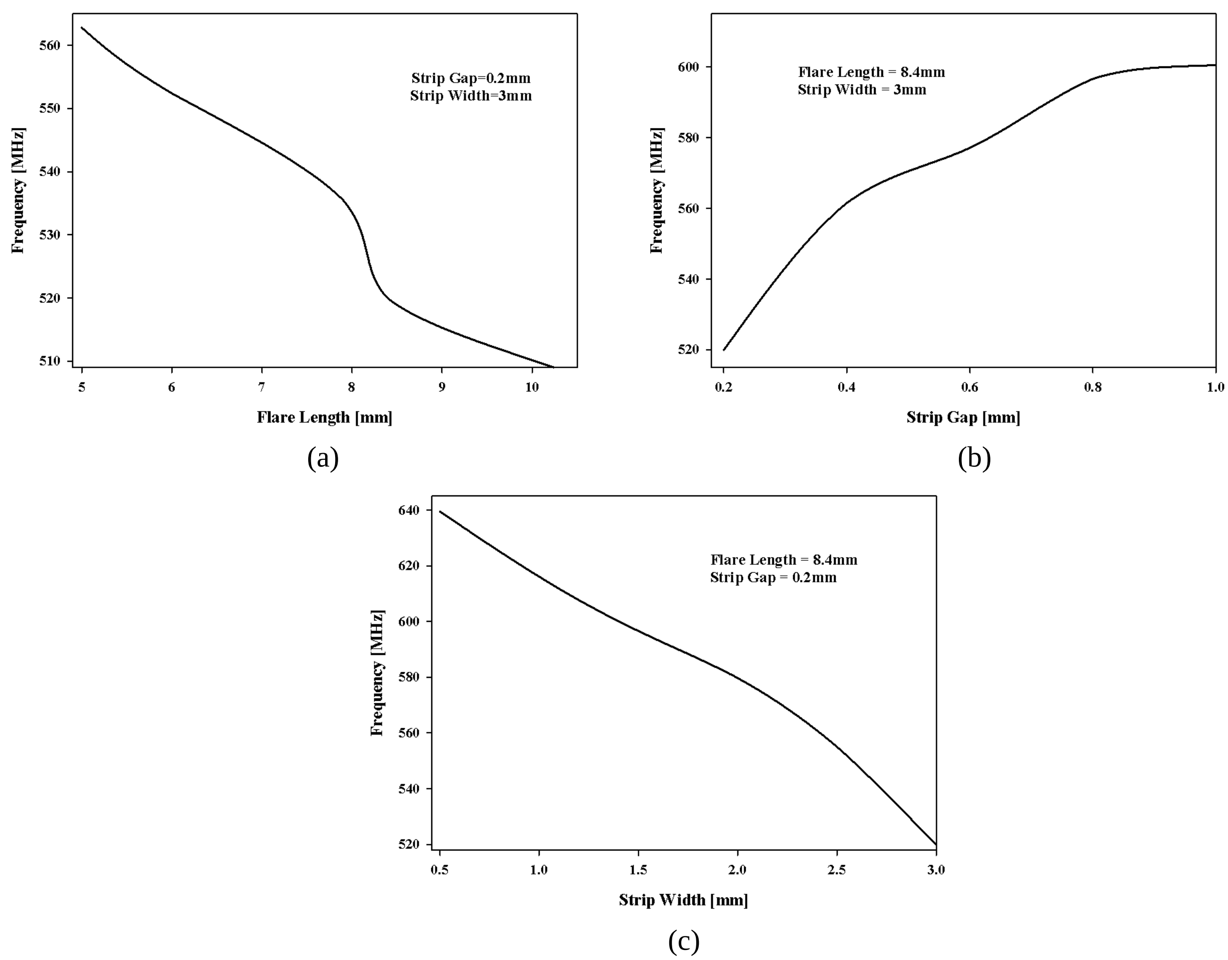

Figure 8. Resonant frequency variation with (a) flare length, (b) strip gap, (c) strip width, $Bl = 11\,\text{mm}$, $Sl = 4\,\text{mm}$, $Iw = 0.3\,\text{mm}$, $h = 1.6\,\text{mm}$, $L = 11.1\,\text{mm}$, $W = 12\,\text{mm}$.

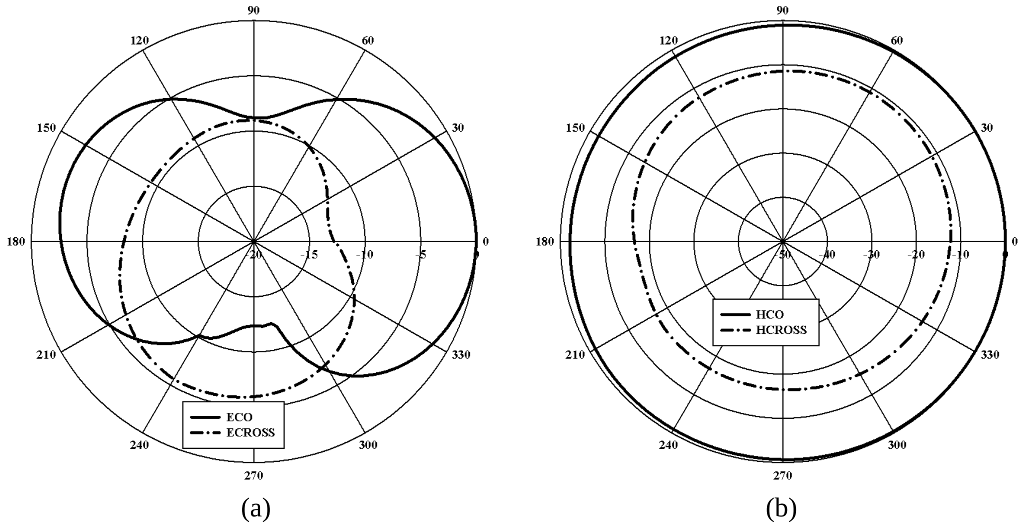

Figure 9. Measured radiation pattern at 503 MHz, (a) E-plane, (b) H-plane, $Bl = 11\,\mathrm{mm}$, $Fl = 8.4\,\mathrm{mm}$, $Sl = 4\,\mathrm{mm}$, $Sw = 3\,\mathrm{mm}$, $Sg = 0.2\,\mathrm{mm}$, $Iw = 0.3\,\mathrm{mm}$, $h = 1.6\,\mathrm{mm}$, $L = 11.1\,\mathrm{mm}$, $W = 12\,\mathrm{mm}$.

are anti-parallel to each other. So an inductor placed across that slot have a shunt effect which makes the chip inductor to represent the shunt inductance (L_L) in the equivalent model of the antenna.

Rigorous parametric analysis has been conducted to find the effect of various antenna parameters on the radiation performance. Figure 7 shows the variation of the resonant frequency with the value of chip inductor. The resonant frequency does decrease with increased inductance value, while the antenna size is maintained the same. The resonant frequency is inversely proportional to the square root of the chip inductance. The effect of flare length (Fl), strip gap (Sg) & strip width (Sw) on the resonant characteristics are shown in Figures 8(a), 8(b) & 8(c) respectively. A lowering in the resonant frequency is obtained when C_R and C_g is increased, which is accomplished by an increase in strip width and/or decrease in strip gap. But this will lead to the re-fabrication of the whole structure. Instead resonant frequency can be tuned by simply changing the value of chip inductor.

The measured radiation pattern of the proposed zeroth order bowtie antenna is shown in Figures 9(a) & 9(b). An omnidirectional radiation pattern is obtained at the zeroth order frequency (503 MHz), since the electric field distribution for $n = 0$ mode does not change much within the bandwidth. The monopolar radiation is maintained over the bandwidth. The cross polarization level for E-plane is 12.8 dB and for the H-plane it is 12.5 dB. The measured peak gain of the antenna using three antenna method is −9.2 dBi and measured radiation efficiency using Wheeler Cap method [21] is 37% at 503 MHz. Both the gain and radiation efficiency stands within the DVB-H specification [22]. The physical area of a circular patch antenna fabricated on the same substrate and operating at the same frequency is 15836.76 mm^2, while that of the proposed antenna is only 133.2 mm^2. Thus a 99.1% reduction in the overall physical area of the structure is obtained compared to circular patch antenna.

5. CONCLUSION

In this paper a novel low profile, extremely compact, zeroth order bowtie antenna for DVB-H application, with less structural complexity, is presented. By loading a chip inductor on one of the bowtie strips a lower resonance independent of the antenna size is obtained. A 99.1% of overall size reduction is achieved compared to a conventional circular patch antenna operating at the same frequency. The operating principle of the antenna is explained in terms of circuit parameters. The antenna exhibits a zeroth order resonance at 503 MHz with −35 dB reflection coefficient and has 3 : 1 VSWR bandwidth of 39 MHz with a gain of −9.2 dBi and radiation efficiency of 37% which are in agreement with the DVB-H specification.

ACKNOWLEDGMENT

The authors acknowledge the University Grant Commission and Department of Science Technology under Government of India for the financial support.

REFERENCES

1. Xiong, J., Z. Ying, and S. He, "A broadband lowprofile patch antenna of compact size with three resonances," *IEEE Trans. Antennas Propag.*, Vol. 57, No. 6, 1838–1843, Jun. 2009.
2. Kramer, O., T. Djerafi, and K. Wu, "Vertically multilayer-stacked Yagi antenna with single and dual polarizations," *IEEE Trans. Antennas Propag.*, Vol. 58, No. 4, 1022–1030, Apr. 2010.
3. Azad, M. Z. and M. Ali, "A miniature implanted inverted-F antenna for GPS application," *IEEE Trans. Antennas Propag.*, Vol. 57, No. 6, 1854–1858, Jun. 2009.
4. Krishna, D. D., M. Gopikrishna, C. K. Aanandan, P. Mohanan, and K. Vasudevan, "Compact wideband Koch fractal printed slot antenna," *Microw. Antennas Propag.*, Vol. 3, No. 5, 782–789, 2009.
5. Sanada, A., C. Caloz, and T. Itoh, "Characteristics of the composite right/left-handed transmission line," *IEEE Microw. Wireless Compon. Lett.*, Vol. 14, No. 2, 68–70, Feb. 2004.
6. Caloz, C. and T. Itoh, *Electromagnetic Metamaterials: Transmission Line Theory and Microwave Applications: The Engineering Approach,* Wiley-IEEE Press, USA, 2006.
7. Liu, W., Z. Zhang, and Z. Feng, "A bidirectional circularly polarized array of the same sense based on crlh transmission line," *Progress In Electromagnetics Research*, Vol. 141, 537–552, 2013.
8. Rennings, A., T. Liebig, S. Abielmona, C. Caloz, and P. Waldow, "Triband and dual-polarized antenna based on composite right/left-handed transmission line," *Proceedings of 37th Eur. Microw. Conf.*, 720–723, Munich, Oct. 9–12, 2007.
9. Lee, C. J., K. M. K. H. Leong, and T. Itoh, "Compact dual-band antenna using an anisotropic metamaterial," *Proceedings of 36th Eur. Microw. Conf.*, 1044–1047, Manchester, Sep. 10–15, 2006.
10. Lee, J. G. and J. H. Lee, "Zeroth order resonance loop antenna," *IEEE Trans. Antennas Propag.*, Vol. 55, No. 3, 994–997, Mar. 2007.
11. Sanada, A., M. Kimura, I. Awai, C. Caloz, and T. Itoh, "A planar zerothorder resonator antenna using a left-handed transmission line," *Proceedings of 34th Eur. Microw. Conf.*, Vol. 3, 1341–1344, Amsterdam, Oct. 12–14, 2004.
12. Lai, A., C. Caloz, and T. Itoh, "Composite right/left-handed transmission line metamaterials," *IEEE Microwave Mag.*, Vol. 5, No. 3, 34–50, Sep. 2004.
13. Wong, K. and S. Chen, "Printed single-strip monopole using a chip inductor for penta-band WWAN operation in the mobile phone," *IEEE Trans. Antennas Propag.*, Vol. 58, No. 3, 1011–1014, Mar. 2010.
14. Kang, T. and K. Wong, "Chip-inductor-embedded small-size printed strip monopole for WWAN operation in the mobile phone," *Microw. Opt. Technol. Lett.*, Vol. 51, No. 4, 996–971, Apr. 2009.
15. Eldek, A. A., A. Z. Elsherbeni, and C. E. Smith, "Wideband microstrip-fed printed bow-tie antenna for phased-array systems," *Microw. Opt. Technol. Lett.*, Vol. 43, No. 2, 123–126, Oct. 2004.
16. Han, W., J. Zhao, and Y. Feng, "Omni-directional microstrip ring antenna based on a simplified left-handed transmission line structure," *International Symposium on Biophotonics, Nanophotonics and Metamaterials*, 455–458, Hangzhou, Oct. 16–18, 2006.
17. Lai, A., S. Member, K. M. K. H. Leong, and T. Itoh, "Infinite wavelength resonant antenna with monopolar radiation pattern based on periodic structures," *IEEE Trans. Antennas Propag.*, Vol. 55, No. 3, 868–876, Mar. 2007.
18. Collin, R. E. and S. Rothschild, "Evaluation of antenna Q," *IEEE Trans. Antennas Propag.*, Vol. 12, No. 1, 23–27, Jan. 1964.

19. Sanada, A., K. Murakami, S. Aso, and H. Kubo, "A via-free microstrip left-handed transmission line," *2004 IEEE MTT-S International Microwave Symposium Digest*, Vol. 1, 301–304, Texas, Jun. 6–11, 2004.
20. Satish, G. N., K. V. Srivastava, A. Biswas, and D. Kettle, "A via-free left-handed Transmission line with radial stubs," *Asia Pacific Microwave Conference, APMC 2009*, 2501–2504, Singapore, Dec. 7–10, 2009.
21. Choo, H., R. Rogers, and H. Ling, "On the wheeler cap measurement of the efficiency of microstrip antennas," *IEEE Trans. Antennas Propag.*, Vol. 53, No. 7, 2328–2332, Jul. 2005.
22. ETSI, "Digital video broadcasting (DVB); DVB-H implementation guidelines," TR 102 377, V1.2.1, Nov. 2005.